AAEC/E402

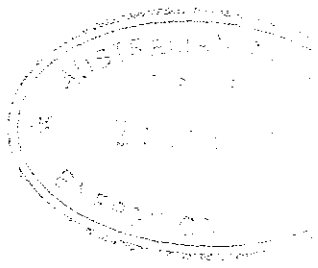

AUSTRALIAN ATOMIC ENERGY COMMISSION

RESEARCH ESTABLISHMENT

LUCAS HEIGHTS

RESONANCE NEUTRON CAPTURE IN THE ISOTOPES OF TITANIUM**

by

B.J. ALLEN
J.W. BOLDEMAN
A.R. de L. MUSGROVE
R.L. MACKLIN*

**Research sponsored in part by ERDA under contract to Union Carbide Corporation

*Oak Ridge National Laboratory, Oak Ridge, Tenn. USA

June 1977

ISBN 0 642 99785 3

AUSTRALIAN ATOMIC ENERGY COMMISSION
RESEARCH ESTABLISHMENT
LUCAS HEIGHTS

RESONANCE NEUTRON CAPTURE IN THE ISOTOPES OF TITANIUM[†]

by
B.J. ALLEN
J.W. BOLDEMAN
A.R. de L. MUSGROVE
R.L. MACKLIN*

ABSTRACT

The neutron capture cross sections of ^{46,47,48,49,50}Ti have been measured from 2.75 to 300 keV with ~0.2 per cent energy resolution. The reduced neutron and radiative widths of the s-wave resonances exhibit correlations which, with the exception of ^{47}Ti, are consistent with the calculated magnitudes of the valence component, assuming that the radiative widths contain an additional uncorrelated part. In ^{47}Ti, a significant correlation is observed for $J=3^-$ resonances, although the calculated valence component is small.

† Research sponsored in part by ERDA under contract to Union Carbide Corporation

* Oak Ridge National Laboratory, Oak Ridge, Tenn. 37830, USA.

National Library of Australia card number and ISBN 0 642 99785 3

The following descriptors have been selected from the INIS Thesaurus to describe the subject content of this report for information retrieval purposes. For further details please refer to IAEA-INIS-12(INIS: Manual for Indexing) and IAEA-INIS-13 (INIS: Thesaurus) published in Vienna by the International Atomic Energy Agency.

CAPTURE; CROSS SECTIONS; GAMMA SPECTRA; KEV RANGE 0-10; KEV RANGE 10-100; KEV RANGE 100-1000; NEUTRON REACTIONS; RESONANCE; S WAVES; TITANIUM 46; TITANIUM 47; TITANIUM 48; TITANIUM 49; TITANIUM 50.

CONTENTS

1. INTRODUCTION

Non-statistical processes in neutron capture are prevalent in the N=28 region where the 3s neutron orbital is just unbound. Low lying states have large 2p single particle components and E1 transitions, after s-wave capture, are predicted by the valence model [Lynn 1968] to be strong. Correlations between the reduced neutron widths and radiative widths of s-wave resonances have been observed [Block *et al.* 1971; Musgrove *et al.* 1976,1977; Allen *et al.* 1976a, 1977; Kenny *et al.* 1977] and resonance γ-ray spectra are seen to be dominated by transitions to the 2p final states [Bird *et al.* 1973].

With the exception of ^{54}Fe [Allen *et al.* 1977], the valence model has been unable to account adequately for the observed radiative widths and γ-ray spectra in the 40-70 mass region. A further 2p-1h process has been invoked in Sc [Allen *et al.* 1976b] and ^{56}Fe [Allen *et al.* 1977] to account for the data. It is of interest then to examine the capture mechanism in the Ti isotopes since the $f_{7/2}$ neutron shell closes at N=28.

The Ti isotopes are of further interest in studies of nucleosynthesis since their genesis is thought to be during explosive oxygen and silicon burning. However, the over-abundances [Woosley *et al.* 1973] of ^{47}Ti and ^{50}Ti suggest an important role for neutron capture, and Maxwellian averaged capture cross sections are therefore required.

The capture cross sections of the Ti isotopes are also of importance for fast reactor and shielding calculations. The present data satisfy, in part, high priority requests given in WRENDA 76-77 [Lessler 1976].

2. MEASUREMENTS AND ANALYSIS

The capture cross section measurements were made at the 40 metre station of the Oak Ridge Electron Linear Accelerator (ORELA). Capture γ-rays were detected by two non-hydrogenous (C_6F_6) liquid scintillators [Macklin & Allen 1971; Allen *et al.* 1973]. Events were weighted according to the observed γ-ray energy to achieve a detector response proportional to the total energy of the capture reaction. A 0.5 mm ^{6}Li glass scintillator, 0.5 metre upstream from the capture sample, operated as a neutron monitor in the transmission mode [Macklin *et al.* 1971]. The Li(n,α) cross section and efficiency perturbations caused by the glass constituents have been previously parameterised [Macklin *et al.* 1975] and the absolute efficiency was determined by the saturated resonance method for the 4.9 eV resonance in gold.

Details of the isotopic targets and run conditions are given in Tables 1 and 2. The five isotopes were first measured as a set (Figure 1) using a fission monitor for overall normalisation to a later $^{6}Li(n,\alpha)$ flux measurement. At a later date, the ^{48}Ti sample was again measured and the ratio of capture areas for eleven isolated resonances in the two ^{48}Ti measurements was found to be 1.08 ± 0.12.

The capture resonances were analysed using a modified version of the ORNL-RPI Monte Carlo code [Sullivan *et al.* 1969]. Breit-Wigner single level theory was used to generate capture and total cross sections, and the observed resonance areas were fitted by an iterative process after subtraction of the multiple-scattering component. The thin sample capture area $A_\gamma = 2\pi^2 \lambda^2 g \Gamma_\gamma \Gamma_n / \Gamma$ is obtained from this area fit. A shape fit can also be used to estimate the neutron width when $\Gamma_n \gtrsim 0.2\ \Gamma_R$, where Γ_R is the energy resolution (typically 0.2-0.3 per cent of the resonance energy). If Γ_n is not known, an assumed value is used to calculate the appropriate self-shielding correction.

A prompt background correction is also made to account for the sensitivity of the detectors to resonance scattered neutrons. For $\ell > 0$ resonances, this correction is negligible, but for s-wave resonances when $\Gamma_\gamma/\Gamma_n < 10^{-4}$, a substantial correction is required. This correction has been deduced from measurements of potential scattering [Allen *et al.* 1973] in C and ^{208}Pb, and resonance capture in many nuclides for energies from 7.6 to 440 keV.

In the case of ^{48}Ti, a multilevel formalism was used to take account of the interference between s-wave resonances observed in the total cross section below 52 keV. Asymmetry is observed in the capture cross section and, as only three γ-rays contribute significantly to radiative decay in this region [Bird *et al.* 1973], a multilevel fit with three γ-ray channels was used to account for the capture cross section. However, the prompt background effect also contributes to the asymmetry and it was not possible to obtain an unambiguous analysis of the data.

3. RESULTS

Capture yields in millibarns are shown for the isotopes of titanium for the energy range 2.7 to 90 keV in Figure 1. Average resonance parameters and capture cross sections are given in Tables 3 and 4, and results for individual nuclides are discussed in the following paragraphs.

(a) ^{46}Ti *(Table 5)*

Shape analysis of the s-wave resonances yields estimates of the neutron widths which, for resonances at 11.06 and 39.20 keV, are in disagreement with transmission results [Farrell *et al.* 1966]. The shape fit to the 11.1 keV resonance is shown in Figure 2 and provides an unambiguous estimate of the neutron width. The transmission value is shown for comparison.

The level density (Figure 3) increases above 70 keV, corresponding to the probable detection of d-wave resonances when the neutron widths exceed the radiative widths. Above 110 keV, the level density decreases as the smaller p-wave resonances are missed.

The p-wave radiative width is deduced for resonances below 70 keV, omitting the smallest values of $g\Gamma_\gamma\Gamma_n/\Gamma$ which may be attributed to d-wave resonances.

(b) ^{47}Ti *(Table 6)*

Shape fits to s-wave resonances permit neutron width determinations which resolve large discrepancies in earlier total cross section measurements [Good *et al.* 1966; Cho *et al.* 1970; Garg *et al.* 1971; Good 1973]. Large discrepancies also occur between the measured s-wave radiative widths and those of Ernst *et al.* [1970]. Above 20 keV, agreement is within 10 per cent, but capture areas differ by factors of two at lower energies (Figure 4).

Two populations of s-wave resonances with different characteristics are readily discernible. Resonances with spin 3^- have twice the neutron strength function of the 2^- resonances, and have radiative widths which are strongly correlated with the corresponding reduced neutron widths.

The average p-wave radiative width is obtained from $\ell > 0$ resonances above 30 keV where it is assumed that $\Gamma_\gamma(p) << \Gamma_n(p)$ in most cases. Below 20 keV, many small values of $g\Gamma_\gamma\Gamma_n/\Gamma$ are observed which are assumed to yield $g\Gamma_n$ as $\Gamma_n << \Gamma_\gamma$. From these resonances a p-wave strength function is obtained.

(c) ^{48}Ti *(Table 7)*

The total cross section data of Garg *et al.* [1971] strongly suggest the presence of an s-wave doorway state in the region 10-50 keV, the local strength function being $10^4 S_0 = 14.5$. The radiative widths of these resonances have large errors resulting from the complexity of the analysis (*i.e.* resonance-resonance interference with large multiple-scattering and prompt background corrections).

Multiple-scattering events account for half the observed yield at 17 keV, and a thin sample run is required to obtain more accurate results. The s-wave resonance parameters for the single and multi-level analyses are given in Table 8, together with the estimated prompt background correction (10^4k) and the recommended radiative widths.

Information on d-wave resonances was obtained as follows. Only $d_{5/2}$ resonances can decay by E1 transitions to the $^{7}/_{2}^{-}$ ground state. It was, therefore, possible to apply a crude pulse height bias at 7.3 MeV to exclude γ-ray transitions to the excited states. The ratios of high bias capture yields to the total yields indicate that certain resonances do have strong ground state components and can therefore be assigned as $d_{5/2}$. One of these, at 39.1 keV, has been identified previously [Broomhall 1972].

(d) ^{49}*Ti (Table 9)*

The s-wave resonances have been identified in several total cross section measurements [Good *et al.* 1966; Cho *et al.* 1970; Garg *et al.* 1970; Good 1973], but substantial differences in energy are observed in the ORELA data. In most cases, the reported neutron widths provide good shape fits to the data, but a substantial discrepancy occurs for the 8.44 keV resonance (Figure 5). The s-wave resonances exhibit significant correlations for both spin values.

Many small resonances ($g\Gamma_\gamma\Gamma_n/\Gamma << 0.1$) were observed, but for the majority of these, their energies and capture areas corresponded to isotopic impurities in the sample.

(e) ^{50}*Ti (Table 10)*

This isotope has N=28 and corresponds to closure of the $f_{7/2}$ neutron shell. As a consequence, the cross section is low and only one s-wave resonance has been assigned [Farrell *et al.* 1966] below 140 keV. Reported s-wave resonances at 146.8 and 186 keV are not observed in capture. Most of the resonances seen in Figure 2 are assigned as isotopic impurities in the sample.

The Ti isotopes are found to exhibit two important properties. The average s-wave radiative widths vary from two to four times the p-wave radiative widths, and significant correlations between the reduced neutron widths and radiative widths of s-wave resonances are observed. These properties are interpreted in Section 4.

4. CAPTURE MECHANISM

The presence of strong transitions to the single particle p-states observed in ^{48}Ti [Broomhall 1972; Bird *et al.* 1973], together with the observation of initial state correlation coefficients, indicates that a valence capture mechanism may be important.

The valence width for an El transition from resonance λ to final state μ is given by [Lane & Mughabghab 1974; Barrett & Terasawa 1975]

$$\Gamma^{V}_{\lambda\mu} = q_{\lambda\mu} \cdot E^{3}_{\gamma} \cdot \theta^{2}_{\mu} \cdot (Z/A)^{2} \cdot \Gamma^{0}_{\lambda n} \quad ,$$

where θ^2_μ is the spectroscopic factor of the final state, Γ^0_n is the s-wave reduced neutron width and $q_{\lambda\mu}$ contains the radial dipole integral and geometric factors for a zero spin target and is dependent on the neutron energy. The reduced valence widths $q_{\lambda\mu}$ were evaluated using the optical model parameters of Moldauer [1963]. The total valence width is obtained by summing over all final states, *i.e.*

$$\Gamma^{V}_{\lambda\gamma} = Q_{\lambda} \cdot \Gamma^{0}_{\lambda n} \quad .$$

An additional spin term is required to calculate valence widths for the non-zero spin (I_α) target nuclides, and can be expressed in terms of the zero spin q value,

$$q_{\lambda}(I_{\alpha}) = \left[\sqrt{(2J_{\lambda}+1)(2J_{\mu}+1)} \begin{Bmatrix} j' & J_{\lambda} & I_{\alpha} \\ J_{\mu} & j'' & 1 \end{Bmatrix} \right] \cdot q_{\lambda}(I_{\alpha} = 0)$$

where j', j" are the initial and final valence neutron spins, and J_λ, J_μ are the spins of the resonance and final state. The calculation is most sensitive to the energies and spectroscopic factors of the low lying states, and the (d,p) results of Kocher & Haeberli [1972] have been used to obtain the valence widths given in Table 11.

(a) ^{48}Ti and ^{49}Ti

Referring to Table 11, only in two cases (the 17.6 keV (^{48}Ti) and 32.43 keV (^{49}Ti) resonances) are the valence estimates found to be in excess of the measured radiative widths. However, in both of these cases large prompt background corrections have been made which could have been overestimated. Other problems associated with the 17.6 keV

analysis have been discussed earlier.

On average, the valence model accounts for over half of the s-wave radiative widths for ^{48,49}Ti. Assuming that the p-wave radiative widths provide an estimate for the statistical component of the s-wave widths, the average residual s-wave component ($\bar{\Gamma}^R_\gamma = \bar{\Gamma}_\gamma(s) - \bar{\Gamma}_\gamma(p)$) is comparable to the valence estimate for these nuclides.

Thermal capture in ^{48,49}Ti is a resonance process and the γ-ray spectra exhibit strong transitions to low lying p-states with large spectroscopic factors. Kopecky [1973] finds final state correlations $\rho[(2J+1)S, I_\gamma/E_\gamma^3]$ of 0.89±0.24 and 0.78±0.26 respectively.

Capture γ-ray spectra for resonances below 74 keV in ^{48}Ti [Broomhall 1972; Bird *et al.* 1973] are similar to those for thermal capture, and confirm the non-statistical nature of the capture mechanism.

While these results support a dominant role for the valence process, the observed initial state correlations $\rho(\Gamma^0_n, \Gamma_\gamma(s)) \sim 0.5$ cannot be explained without invoking a further capture mechanism. This mechanism must be uncorrelated with the reduced neutron widths, but favours transitions to strong, single-particle final states. The resonance radiative width can therefore be written as

$$\Gamma_{\lambda\gamma} = \sum_\mu [(\Gamma^V_{\lambda\mu})^{\frac{1}{2}} + (\Gamma^U_{\lambda\mu})^{\frac{1}{2}}]^2 + \Gamma^S_{\lambda\gamma} \quad ,$$

where $\Gamma^U_{\lambda\mu}$ denotes the uncorrelated component of the radiative width which interferes with the valence transitions to the single-particle final states μ. We assume that the statistical component $\Gamma^S_{\lambda\mu}$ is negligible for these states, and the variance of $\Gamma^S_{\lambda\gamma}$ is relatively small.

The observed correlation coefficient is given by

$$\rho(\Gamma^0_n, \Gamma_\gamma(s)) = \frac{\bar{\Gamma}^V_\gamma}{\bar{\Gamma}^V_\gamma + \bar{\Gamma}^U_\gamma} \sqrt{\frac{\sigma^2_V}{\sigma^2_V + \sigma^2_U + \sigma^2_S}}$$

and, if the variance $\sigma^2_V >> \sigma^2_U + \sigma^2_S$, then for $\rho \sim 0.5$ the average uncorrelated component is comparable to the average valence width.

We conclude, therefore, that the average statistical width is less than the average p-wave radiative width, indicating that a substantial non-statistical component is also present for p-wave

resonances. Capture γ-ray spectra for p-wave resonances are needed to confirm this prediction. In ^{56}Fe p-wave resonances show strong M1 transitions to the single-particle final states, thus supporting this contention.

The nature of the uncorrelated component has been explored in ^{45}Sc [Allen *et al.* 1976b] and ^{56}Fe [Allen *et al.* 1976a, 1977], and has been attributed to the excitation of 2p-1h states. These states are of the type $|2p_{3/2}, 2p_{1/2}, 2s_{1/2}^{-1}; 1/2^+\rangle$ or $|2p_{3/2}, 2p_{1/2}, 1d_{3/2}^{-1}; 1/2^+\rangle$ which decay by E1 transitions to final states with large 2p single-particle strength. Enhanced M1 transitions can result from the decay of states like $|2p_{3/2}, 1f_{5/2}, 1f_{7/2}^{-1}; 3/2^-\rangle$ to the low lying 2p states.

(b) ^{46}Ti

The valence component in ^{46}Ti is found to be a smaller fraction of the s-wave radiative width than in ^{48,49}Ti, but the above discussion still applies.

(c) ^{47}Ti

Only the 3^- resonances are strongly correlated, a result which relates in part to the larger s-wave neutron strength function for this sequence. However, the calculated valence component is relatively small (Table 3) and, in order to account for the observed correlation, the uncorrelated component must be even smaller. The absence of correlations for the 2^- sequence implies that the uncorrelated component is large with respect to the valence amplitude.

5. CONCLUSIONS

The neutron capture cross sections of the isotopes of titanium have been measured and resonance parameter sets obtained. The s-wave data exhibit correlations between the reduced neutron and radiative widths, and p-wave radiative widths are found to be up to four times smaller than s-wave values. The data indicate the dominance of single-particle mechanisms, but the valence process alone cannot account for either the magnitude of the radiative widths or the observed correlations. Another mechanism is required which is uncorrelated with the neutron widths, adding further support to the role of 2p-1h states in the 3s mass region.

6. REFERENCES

Allen, B.J., Macklin, R.L., Winters, R.R. & Fu, C.Y. [1973] - *Phys. Rev.*, C8:1504.

Allen, B.J., Musgrove, A.R. de L., Boldeman, J.W., Kenny, M.J. & Macklin, R.L. [1976a] - *Nucl. Phys.*, A269:408.

Allen, B.J., Kenny, M.J., Barrett, R.F. & Bray, K.H. [1976b] - *Phys. Lett.*, 61B:161.

Allen, B.J., Musgrove, A.R. de L., Boldeman, J.W. & Macklin, R.L. [1977] - AAEC/E403; also *Nucl. Phys.* (In press - abridged version).

Barrett, R.F. & Terasawa, T. [1975] - *Nucl. Phys.*, A240:445.

Bird, J.R., Allen, B.J., Bergqvist, I. & Biggerstaff, J.A. [1973] - *Nucl. Data Tables*, 11:434

Block, R.C., Stieglitz, R.G. & Hockenbury, R.W. [1971] - Proc. Conf. Neutron Cross Sections and Technology, Knoxville. CONF-710701, p.889.

Broomhall, G.J. [1972] - *Aust. J. Phys.*, 25:9

Cho, M., Frohmer, F.H., Kazerouni, M., Muller, K.N. & Rohr, G. [1970] - Proc. Conf. on Nuclear Data for Reactors, Helsinki. IAEA-CN-26/127, p.619.

Ernst, A., Frohner, F.H. & Kompe, D. [1970] - Proc. Conf. on Nuclear Data for Reactors, Helsinki. IAEA-CN-26/11, p.633.

Farrell, J.A., Bilpuch, E.G. & Newson, H.W. [1966] - *J. Appl. Phys.*, 37:367.

Garg, J.B., Rainwater, J. & Havens, W.W. Jnr [1971] - *Phys. Rev.*, C3:2447.

Good, W.M., Paya, D., Wagner, R. & Tamura, T., [1966] - *Phys. Rev.*, 151:912.

Good, W.M. [1973] - Cited in Mughabghab & Garber [1973].

Kenny, M.J., Allen, B.J., Musgrove, A.R. de L., Macklin, R.L. & Halperin, J. [1977] - AAEC/E400.

Kocher, D.C. & Haeberli, W., [1972] - *Nucl. Phys.*, A196:225.

Kopecky, J. [1973] - RCN-73-094.

Lane, A.M. & Mughabghab, S.F. [1974] - *Phys. Rev.*, C10:414.

Lessler, R.M. (ed.) [1976-77] - World Request Nuclear Data. IAEA, INDC(SEC) - 55/URSF.

Lynn, J.E. [1968] - Theory of Neutron Resonance Reactions. Clarendon Press, Oxford.

Macklin, R.L. & Allen, B.J. [1971] - *Nucl. Instrum. Methods*, 91:565.

Macklin, R.L., Hill, N.W. & Allen, B.J. [1971] - *Nucl. Instrum. Methods*, 96:509.

Macklin, R.L., Halperin, J. & Winters, R.R. [1975] - *Phys. Rev.*, C11:1270.

Moldauer, P.A. [1963] - *Nucl. Phys.*, 47:65.

Mughabghab, S.F. & Garber, D.I. [1973] - BNL-325, Vol 1 (3rd ed.).

Muller, K.N. & Rohr, G. [1971] - *Nucl. Phys.*, A164:97.

Musgrove, A.R. de L., Allen, B.J., Boldeman, J.W., Chan, D.M.H. & Macklin, R.L. [1976] - *Nucl. Phys.*, A259:365.

Musgrove, A.R. de L., Allen, B.J., Boldeman, J.W., Chan, D.M.H. & Macklin, R.L. [1977] - *Nucl. Phys.*, (In press).

Sullivan, J.G., Warner, G.G., Block, R.C. & Hockenbury, R.W. [1969] - Rensselaer Polytechnic Institute report RPI-328-155.

Woosley, S.E., Arnett, W.D. & Clayton, D.D. [1973] - *Astrophys. J. Suppl. Ser.*, 26:23.

TABLE 1

TARGET AND RUN PARAMETERS

Isotope	Target	Weight (g)	%	Thick-ness (cm)	atom $barn^{-1}$ x 10^3	Pulse Width (ns)	Average Power (kW)	No. of Bursts x 10^6
^{46}Ti	TiO_2	6.60	85.90	0.42	6.48	8	5	40.5
^{47}Ti	TiO_2	3.33	80.10	0.20	3.01	8	5	38.8
^{48}Ti	TiO_2	24.66	99.10	0.86	13.63	8	5	43.7
						30	38	774
^{49}Ti	TiO_2	13.15	76.57	0.93	11.09	8	5	38.0
^{59}Ti	TiO_2	24.43	67.72	0.88	9.00	8	5	47.3

TABLE 2

ISOTOPIC ABUNDANCES (%)

Isotope	^{46}Ti	^{47}Ti	^{48}Ti	^{49}Ti	^{50}Ti
^{46}Ti	85.90	1.56	10.70	0.84	1.03
^{47}Ti	1.87	80.1	15.8	1.11	1.1
^{48}Ti	0.15	0.32	99.10	0.22	0.22
^{49}Ti	1.75	1.64	17.98	76.57	2.06
^{50}Ti	2.71	2.48	24.1	2.99	67.72

TABLE 3

AVERAGE RESONANCE PARAMETERS

A	ℓ,J	D_ℓ [a] (keV)	$10^4 S_\ell$	E_{max} (keV)	$\bar{\Gamma}_\gamma(\ell)$ (eV)	S.D. [b]	$\bar{\Gamma}^V_\gamma$ (eV)	N_{obs} [c]	$\rho(\Gamma^0_n, \Gamma_\gamma)$	S.D. [d]	$\bar{\Gamma}^R_\gamma$ [e] (eV)	$\bar{\Gamma}^V_\gamma/\bar{\Gamma}^R_\gamma$	$\bar{\Gamma}^V_\gamma/\bar{\Gamma}_\gamma$(s)
^{46}Ti	0	20	2.4	186	1.68	1.10	0.53	6	0.78	0.45	1.28	0.41	0.32
	1			<70	0.40	0.14		15					
	ℓ>0	1.83		186	0.47	0.24		67					
^{47}Ti	0	2.2	3.2	76	1.27	0.63	0.13	30	0.38	0.18	0.53	0.25	0.10
	$0,2^-$	4.8	1.8	76	1.35	0.61		13	0.10	0.27			
	$0,3^-$	4.2	3.8	76	1.24	0.65	0.18	16	0.65	0.25	0.68	0.19	0.13
	1	1.1	1.7	<16				12					
	(1)	0.64		>30	0.74	0.24		54					
^{48}Ti	0	19.0	5.3	200	1.34	0.83	0.83	10	0.42	0.33	1.01	0.82	0.60
	(1)	4.88		300	0.33	0.23		44					
	$2,5/2^+$			300	0.54	0.36		10					
^{49}Ti	0	5.1	2.8	80	0.82	0.31	0.35	12	0.66	0.29	0.43	0.81	0.43
	1	1.52		80	0.39	0.26		43					
^{50}Ti	0	(150)			1.10	0.30	0.23	1					
	(1)	8.6		300	0.45	0.56		18					

a) Level density obtained from linear fit to the steepest, consistent slope in cumulative level spacing histograms.

b) Standard deviation of distribution.

c) Actual number of observed resonances

d) Standard deviation of distribution of correlation coefficients calculated by Monte Carlo sampling from an uncorrelated population for the appropriate sample size.

e) $\bar{\Gamma}^R_\gamma = \bar{\Gamma}_\gamma(s) - \bar{\Gamma}_\gamma(p)$

TABLE 4

AVERAGE CAPTURE CROSS SECTIONS (mb)

	$\frac{\langle\sigma\cdot v\rangle}{v_T}$ [a]	$\sum \frac{A_\gamma}{E}$ [a]	3-10	10-20	20-30	30-40	40-50	50-60	60-70	70-80	80-90	90-100	100-150	150-200	200-250	250-300
^{46}Ti	26.9	91.3		63.6	14.0	21.5	36.2	9.76	24.1	12.7	27.1	20.3	16.4			
S.D.	3.2	11.0		7.6	1.7	2.7	4.7	1.21	3.9	1.6	3.3	2.5	2.1			
^{47}Ti	65.5 [b]	636	256	168	85.8	33.2	70.8	50.4	45.1							
S.D.	7.7	76	18	20	70.6	4.1	9.5	6.3	5.6							
^{48}Ti	29.7	86.5	1.87	79.0	28.4	33.1	4.78	13.6		11.9	11.8	5.91	4.90	4.37	4.23	5.81
S.D.	4.9	21.4	0.09	36.4	6.0	9.4	0.28	7.4		0.6	0.6	0.30	0.25	0.23	0.23	0.30
^{49}Ti	22.5 [b]	144.0	64.8	12.2	33.5	28.6	7.94	13.8	10.3	11.4						
S.D.	2.1	17.0	5.6	1.5	4.2	3.6	0.99	2.2	1.3	1.8						
^{50}Ti	4.0	8.5		3.81				10.1	5.30	17.3	3.93	3.34	0.54		0.25	1.3
S.D.	0.5	1.1		0.46				2.8	0.65	2.1	0.57	0.46	0.08		0.10	0.2

a) $\frac{\langle\sigma\cdot v\rangle}{v_T}$ is the Maxwellian averaged capture cross section at 30 keV.

$\sum \frac{A_\gamma}{E}$ is the resonance component of the resonance integral above 2.7 keV.

b) Cut-off at 76 keV.

TABLE 5

^{46}Ti RESONANCE PARAMETERS

E_n [a] (keV)	$g\Gamma_\gamma\Gamma_n/\Gamma$ [b] (eV)	$g\Gamma_n$ [c] (eV)	ℓ [d]	J^π [d]	Γ_n [e] (eV)	Γ_n [f] (eV)	$g\Gamma_n$ [g] (eV)
3.990	0.0051						
8.265	0.0036 (12)						
11.06	0.49	80 (15)	0	$1/2^+$	230		230 (50)
12.32	0.47	(2)					
13.72	0.39	(2)					
18.18	[b] $g\Gamma_n$ = 0.044 (4)						
19.39	0.70						
21.24	0.51	10 (5)					
24.06	[b] $g\Gamma_n$ = 0.057 (5)						
28.77	0.11 (5)						
34.00	0.14 (6)						
34.10	0.36						
35.22	0.65						
39.20	0.67 (7)	250 (50)	0	$1/2^+$	550		550 (80)
42.29	0.39						
42.85	0.92						
44.52	0.44						
47.40	0.61						
48.70	1.02 (20)	1500 (300)	0	$1/2^+$	1300	1750	1500 (200)
49.37	0.52						
55.67	0.49						
56.66	0.18 (3)						
59.27	0.65						
61.07	0.20 (3)						
63.20	1.96 (40)	3500 (700)	0	$1/2^+$	3000	1660	3500 (400)
68.05	0.53 (3)						
68.94	1.00						
70.85	0.51 (4)						
71.6			0	$1/2^+$	120		

TABLE 5 (cont'd)

E_n [a] (keV)	$g\Gamma_\gamma\Gamma_n/\Gamma$ [b] (eV)	$g\Gamma_n$ [c] (eV)	ℓ [d]	J^π [d]	Γ_n [e] (eV)	Γ_n [f] (eV)	$g\Gamma_n$ [g] (eV)
75.22	0.69						
77.02	0.35 (4)						
78.32	0.69 (7)						
80.77	0.78 (4)	40 (10)					
81.61	0.66						
81.72	0.67						
84.52	0.84 (6)						
87.07	0.98						
87.40	0.69						
87.63	0.73						
90.55	0.73 (6)						
91.20	1.42						
92.90	0.96 (11)						
94.30	0.73						
99.45	0.57						
99.8			0	$1/2^+$	70		
100.0	3.70 (70)	4800 (900)	0	$1/2^+$	4800		4800 (500)
101.5	0.88 (11)						
105.6	1.66	(70)					70
106.4	0.84 (5)						
106.8	0.64 (4)						
107.4	0.68 (7)						
108.3	0.60 (9)						
109.4	0.94 (18)	(166)					
111 (1)							166
113.6	1.06						
114.8	0.99 (5)	(106)					106

(Continued)

TABLE 5 (cont'd)

E_n [a] (keV)	$g\Gamma_\gamma\Gamma_n/\Gamma$ [b] (eV)	$g\Gamma_n$ [c] (eV)	ℓ [d]	J^π [d]	Γ_n [e] (eV)	Γ_n [f] (eV)	$g\Gamma_n$ [g] (eV)
117 (1)							93
119.8	0.61 (4)						
120.2	0.92	(48)					48
124.5	1.16	(30)					30
128.7	1.42	(84)				55	84
132.6	0.90 (9)	(120)					120
133.5	1.28						
135.8	1.12 (22)	(334)					334
142.0			0	$1/2^+$		1330	
143.5	2.12	(179)					179
146.6	0.86	(153)					153
148.8						1700	
150.6	0.72						
154.0	2.93	(192)					192
157.1	2.89 (20)	(212)					212
158.0							160
160.3	1.85						376
166.0	0.83 (12)						
167.4	2.02 (30)	(175)					175
170.0	1.65 (17)						
171.0						900	
172.6	1.40 (20)						213
174.5	1.12 (22)						72
178.9	2.20 (30)	1300 (400)	0	$1/2^+$	13000	6530	1300 (260)
181.5	0.75 (23)						
182.9	1.39 (20)						
185.2	2.40 (24)		0	$1/2^+$			3500 (500)
186.2	2.00 (30)						

TABLE 5 (cont'd)

a) Systematic energy error 0.2%. Relative energy error $\lesssim$ 0.1% unless the least significant error is given in parentheses.

b) Error in least significant figure is given in parentheses if > 5% (e.g. 2.05 (110) ≡ 2.05±1.10). Normalisation error of 12% is not included.

c) Unless specified, $g\Gamma_n$ = 5 eV is assumed below 110 keV, $g\Gamma_n$ = 50 eV above. Bracketed values are assumed. Least significant error given in parentheses.

d) s-wave assignments from Farrell *et al.* [1966]; Good *et al.* [1966] and Mughabghab & Garber [1973].

e) Γ_n values from Farrell *et al.* [1966].

f) Γ_n values from Garg *et al.* [1971].

g) $g\Gamma_n$ values from Mughabghab & Garber [1973].

TABLE 6

^{47}Ti RESONANCE PARAMETERS

E_n [a] (keV)	$g\Gamma_\gamma\Gamma_n/\Gamma$ [b] (eV)	g	Γ_n [c] (eV)	ℓ [d]	J^π [d]	Γ_γ (eV)	Γ_n [e] (eV)	Γ_n [f] (eV)	Γ_n [g] (eV)	Γ_γ [h] (eV)
3.090	0.63	0.58	100 (20)	0	3^-	1.09	117 (35)	134 (6)		2.0 (2)
4.105	0.031					(0.85)				
4.192	0.25	0.58	2 (1)	0	3^-	0.53		2.8 (14)		
4.539	0.034					(0.85)				
6.167	0.10					(0.85)				
7.550	0.058					(0.85)				
8.130	0.25	0.42	40 (10)	0	2^-	0.62			66 (7)	1.4 (3)
8.346	0.57	0.42	100 (20)	0	2^- / 3^-	1.43	98 (30)	280 (20)	147 (15)	2.0 (4)
8.880	0.085					(0.85)				
9.103	0.063					(0.85)				
10.09	0.043					(0.85)				
10.54	0.68	0.58	56 (10)	0	3^-	1.21	60 (20)		58 (6)	1.6 (2)
12.12	0.73	0.58	120 (20)	0	3^-	1.29	79 (24)		120 (12)	2.1 (5)
12.0 12.14	0.37	0.42	22 (8)	0	2^-	0.92			22 (2)	
12.37	0.13 (1)					(0.85)				
12.83	0.77	0.42	156 (20)	0	2^-	1.87	83 (25)		175 (18)	2.5 (5)
13.15	0.010 (3)					(0.85)				
15.07	0.038 (6)					(0.85)				
16.36	0.52	0.58	300 (50)	0	3^-	0.93	184 (55)		396 (40)	2.0 (4)
16.59	0.21									
16.81	0.26									
17.42	0.69	0.42	40 (10)	0	2^-	1.75			50 (5)	2.0 (3)
18.26	0.20									
18.82	0.31									
19.09	0.54	0.58	20 (5)	0	3^-	0.98			20 (2)	2.5 (5)

TABLE 6 (cont'd)

E_n [a] (keV)	$g\Gamma_\gamma\Gamma_n/\Gamma$ [b] (eV)	g	Γ_n [c] (eV)	ℓ [d]	J^π [d]	Γ_γ (eV)	Γ_n [e] (eV)	Γ_n [f] (eV)	Γ_n [g] (eV)	Γ_γ [h] (eV)
20.07	0.41									
20.23	0.18		0.6			(0.85)				
20.4							708 (212)			
20.82	0.11		0.3			(0.85)				
21.29	0.61	0.42	62 (10)	0	2^-	1.50			62 (6)	1.7 (3)
21.93	0.044 (6)		0.097			(0.85)				
23.22	0.046 (9)		0.10			(0.85)				
23.76	0.009 (7)		0.02			(0.85)				
24.13	0.40 (0.5)		15 (5)			0.84				
24.44	0.26									
24.49	0.30									
24.75	0.47									
25.64	0.29									
26.37	0.21									
27.12					2^-				111 (11)	
27.20	1.46	0.58	860 (100)	0	3^-	2.56			957 (100)	2.70 (35)
28.30	0.031(22)					(0.85)				
30.23	0.33	0.42	65 (20)	0	2^-	0.78	79 (24)		74 (7)	0.85 (10)
31.5							504 (150)			
31.85	0.13									
32.26	0.48									
32.61	0.35 (4)	0.42	600 (100)	0	2^-	0.85			599 (60)	0.92 (15)
33.94	0.24 (2)									
36.1							202 (60)			
37.04	0.36 (6)	(0.5)	500 (100)	0		0.73				0.92 (20)
37.0							200 (60)			
37.75	0.31									

(Continued)

TABLE 6 (cont'd)

E_n [a] (keV)	$g\Gamma_\gamma\Gamma_n/\Gamma$ [b] (eV)	g	Γ_n [c] (eV)	ℓ [d]	J^π [d]	Γ_γ (eV)	Γ_n [e] (eV)	Γ_n [f] (eV)	Γ_n [g] (eV)	Γ_γ [h] (eV)
38.12	0.34	0.58	100 (50)	0	3^-	0.59			80 (8)	0.58 (10)
39.17	0.14 (2)									
40.12	0.24 (2)									
40.55	1.18	0.58	700 (200)	0	3^-	2.03	369 (110)		692 (70)	2.00 (25)
40.81	0.16 (2)									
41.06	0.12 (1)	0.42	58 (30)	0	2^-	0.28	268 (80)		58 (6)	0.35 (15)
42.08					3^-			270 (50)	881 (90)	
42.36	0.92 (18)	0.42	400 (100)	0	2^-	2.26	555 (167)		582 (60)	2.40 (35)
43.38	0.32 (3)									
43.60	0.12									
43.81	0.11 (1)									
43.98	0.33									
44.43	0.37 (4)									
46.30	1.46 (19)	0.58	300 (100)	0	3^-	2.53	484 (145)		706 (70)	2.75 (40)
46.91	0.19 (6)									
47.78	0.23 (3)									
47.92	0.35 (4)									
48.0							221 (66)			
48.34	0.034 (21)					(0.85)				
49.02	0.18 (1)									
49.33	1.04 (9)	0.58	280 (100)	0	3^-	1.82			315 (32)	1.8 (4)
50.3							370 (110)			
51.03	0.30 (2)									
51.39	0.73 (5)	0.58	230 (80)	0	3^-	1.26			180 (18)	
51.9							94 (30)			
52.13	0.40 (3)									
52.38	0.28 (3)									

TABLE 6 (cont'd)

E_n [a] (keV)	$g\Gamma_\gamma\Gamma_n/\Gamma$ [b] (eV)	g	Γ_n [c] (eV)	ℓ [d]	J^π [d]	Γ_γ (eV)	Γ_n [e] (eV)	Γ_n [g] (eV)
53.75	0.52 (4)							
54.0							223 (66)	
54.75	0.52							
54.91	0.19 (2)							
55.13	0.25 (3)							
55.39	0.31	0.58	300 (100)	0	3^-	0.53		276 (28)
55.44	0.28 (3)							
56.2							528 (160)	
56.57	0.12 (4)							
56.75	0.28 (4)							
57.52	0.49 (5)							
57.56	0.70 (21)	0.58	800 (200)	0	3^-	1.20		859 (86)
57.72	0.35 (4)							
58.15	0.14 (4)							
58.45	0.49							
59.15	0.18 (2)							
60.45	0.57 (6)	0.42	70 (20)	0	2^-	1.40		89 (9)
60.66	0.48 (5)							
61.88	0.67 (9)	0.42	180 (50)	0	2^-	1.63		213 (21)
62.07	0.49 (7)							
62.32	0.39 (8)							
62.64	0.35 (7)							
63.20	0.27 (8)							
63.40	0.35 (6)	0.58	110 (30)	0	3^-	0.60		97 (10)
63.57	0.17 (4)							
64.20	0.35 (5)	0.58	60 (20)	0	3^-	0.61		53 (5)
65.32	0.38 (4)							

(Continued)

TABLE 6 (cont'd)

E_n [a] (keV)	$g\Gamma_\gamma\Gamma_n/\Gamma$ [b] (eV)	g	Γ_n [c] (eV)	ℓ [d]	J^π [d]	Γ_γ (eV)	Γ_n [g] (eV)
65.32	0.38 (4)						
65.52	0.40						
66.39	0.31 (5)						
67.07	0.43						
67.65	0.45 (6)						
68.60	0.19 (3)						
68.95	0.28 (5)						
69.87	0.23 (4)						
70.02	0.34 (6)						
71.05	0.42						
71.50	0.26 (5)						
71.88	0.23 (5)		<150	0	3^-		490 (50)
72.47	0.36 (6)						
72.62	0.18 (3)						
72.85	0.42						
73.80	0.29 (9)		100 (40)			0.58	
74.75	0.95	0.42	110 (30)	0	2^-	2.34	128 (13)

[a] Systematic energy error 0.2%. Relative energy error $\lesssim$ 0.1 unless the least significant error is given in parentheses.

[b] Error in least significant figure is given in parentheses if > 5% (e.g. 2.05 (110) ≡ 2.05±1.10). Normalisation error of 12% is not included.

[c] Unless specified, g=0.5 and Γ_n ~ 1 eV below 50 keV and 5 eV above.

[d] (ℓ,J) assignments taken from Good *et al.* [1966] and Cho *et al.* [1970].

[e] Γ_n values from Good *et al.* [1966].

[f] Γ_n values from Garg *et al.* [1971].

[g] Γ_n values from Cho *et al.* [1970].

[h] Γ_γ values from Ernst *et al.* [1970].

TABLE 7

^{48}Ti RESONANCE PARAMETERS

E_n [a] (keV)	$g\Gamma_n\Gamma_\gamma/\Gamma$ [b] (eV)	$g\Gamma_n$ [c] (eV)	ℓ [d]	J^π [d]	Γ_n [e] (eV)	Γ_n [f] (eV)	Γ_n [g] (eV)
6.688	0.021	0.021	2				
11.49	0.30	(3)					
13.42	0.38	(3)					
17.6	2.3 (20)	7000 (1000)	0	$^1/_2{}^+$	8710	7000	8430
21.61	0.19	(5)					
22.1	0.80 (30)	250 (100)	0	$^1/_2{}^+$	650	400	780
23.96	0.52	(5)					
36.8	2.50 (80)	900 (300)	0	$^1/_2{}^+$	1250	1500	1300
39.17	0.38	(24)	2	$^5/_2{}^+$			
42.01	0.088	0.088	2				
42.33	0.39	(10)					
51.9	1.40 (90)	1600 (400)	0	$^1/_2{}^+$	2360	2500	2400
56.48	0.28	(10)					
71.30	0.40	(20)					
74.67	0.35	220 (50)	0	$^1/_2{}^+$	150	-	150
76.51	0.40	(20)					
79.73	0.98	(30)					
80.32	0.55	(30)					
83.4	0.61 (10)	200 (50)	0	$^1/_2{}^+$	130	500	120
85.38	0.25	(30)					
87.37	1.07	(30)					
97.56	1.35	(60)	2	$^5/_2{}^+$			
106.9	0.67	(30)					
113.6	1.72	(30)					
116.5			0	$^1/_2{}^+$		1120	
119.2	0.52	200 (50)	0	$^1/_2{}^+$	200		200
120.7	0.80	(30)					

(Continued)

TABLE 7 (cont'd)

E_n [a] (keV)	$g\Gamma_n\Gamma_\gamma/\Gamma$ [b] (eV)	$g\Gamma_n$ [c] (eV)	ℓ [d]	J^π [d]	Γ_n [e] (eV)	Γ_n [f] (eV)	Γ_n [g] (eV)
122.1	0.42	(30)					
131.5	Not observed		0	$1/2^+$		1690	
133.0			0	$1/2^+$	160		200
133.9	0.38 (5)	(30) [h]					
135.4	0.77	(30)					
136.5	Not observed					300	
141.0	0.86	(30)					
142.3	0.58	(30)					
142.8	0.47	(30)					
145.4	0.22 (4)	(30)					
153.7	2.75	430 (80)	0	$1/2^+$	430	800	250
161.5	0.24 (5)	(90)					
166.4	1.29 (13)	(270)	2	$5/2^+$			
167.3	0.62 (5)	(90)					
184.9	0.78 (7)	(40)					
185.4	1.26 (40)	(650)	0	$1/2^+$	760	650	650
186.7	0.19 (5)	(40)					
188.0	0.62 (7)	(40)					
190.0			0	$1/2^+$		3000	
191.0			0	$1/2^+$	2890		
191.4	0.89 (7)	2000 (500)	0	$1/2^+$			
192.4			0	$1/2^+$			3000
195.2	0.70 (6)	130(40)					
198.6	0.23 (8)	(40)					
202.8	0.82 (8)	(40)					
205.6	3.9 (4)	(120)	2	$5/2^+$			

TABLE 7 (cont'd)

E_n [a] (keV)	$g\Gamma_n\Gamma_\gamma/\Gamma$ [b] (eV)	$g\Gamma_n$ [c] (eV)	ℓ [d]	J^π [d]	Γ_n [e] (eV)	Γ_n [f] (eV)	Γ_n [g] (eV)
213.0	1.42 (11)	(40)	2	$^5/_2^+$			
217.8	0.96 (20)	(40)					
221.4	0.50 (8)	(40)					
226.2	0.57 (9)	(50)					
229.2	0.36 (10)	(50)					
230.8	0.82 (12)	(150)	2	$^5/_2^+$			
233.8	1.05 (14)	(50)					
245.3	0.58 (12)						
247.0 [f]	<1.0		0	$^1/_2^+$		8500	
250.5	2.08 (16)	300 (80)					
252.5	1.75 (18)	(150)	2	$^5/_2^+$			
259.3	1.70 (14)	(50)					
263.5	0.71 (8)	(50)					
266.4	1.53 (16)	(60)					
266.0			0	$^1/_2^+$		4000	
270.0 [f]	<1.0		0	$^1/_2^+$			
273.0	1.68 (8)						
278.9	0.51 (15)	(60)					
280.4	1.26 (15)	(60)					
284.3	0.78 (20)	(60)					
287.0	1.07 (22)	(60)					
290.7	2.08 (12)	(60)					
292.4	3.22	(180)	2	$^5/_2^+$			

[a] Systematic energy error 0.2%. Relative energy error $\leq$0.1% unless the least significant error is given in parentheses.

[b] Error in least significant figure is given in parentheses if >5% (e.g. 2.05 (110) $\equiv$ 2.05±1.10). Normalisation error of 12% is not included.

[c] $g\Gamma_n$ values in parentheses are assumed with g=1. When $\Gamma_n \ll \Gamma_\gamma$, Γ_γ = 1 eV is assumed.

(Continued)

TABLE 7 (cont'd)

d) s-wave assignments from [Farrell *et al.* [1966], Garg *et al.* [1971] and Muller & Rohr [1971]. d-wave assignments from high bias ratios.

e) Γ_n values from Garg *et al.* [1971].

f) Γ_n values from [Farrell *et al.* [1966].

g) Γ_n values from Muller & Rohr [1971].

h) Γ_n < 80 eV.

TABLE 8

s-WAVE PARAMETERS IN ^{48}Ti BELOW 52 keV

E_n (keV)	Γ_n (eV)	Single level Γ_γ (eV)	Multi-level Γ_γ (eV)	$10^4 k$ (a)	$k\Gamma_n$ b) (eV)	Γ_γ a) (eV)
16.3	7000	3.2	1.3	2.0	1.74	$2.3^{+1.5}_{-2.0}$
22.0	250	0.9	1.1	2.0	0.13	0.8±0.3
36.6	900	3.8	3.8	10.0	1.3	2.5±0.8
51.9	1600	2.3	2.3	4.0	0.9	1.4±0.9

a) $\Gamma_\gamma = \Gamma_{\gamma(obs)} - k\Gamma_n$

b) Γ_n values from Garg *et al.* [1971].

TABLE 9

^{49}Ti RESONANCE PARAMETERS

E_n [a] (keV)	$g\Gamma_\gamma\Gamma_n/\Gamma$ [b] (eV)	g [c]	Γ_n [d] (eV)	ℓ	J [c]	Γ_γ [e] (eV)	$2g\Gamma_n$ [f]	Γ_n [g]	Γ_n [h]
3.827	0.29		185 (20)	0	4	0.52	225 (25)		
4.796	0.010		0.021			(0.5)			
7.637	0.060		(2)			0.13			
8.435	0.25	(0.438)	250 (40)	0	(3)	0.58	100 (20)		
13.18	0.028		0.065			(0.5)			
13.98	0.035		0.081			(0.5)			
14.78	0.16		(2)						
17.06	0.034		0.078			(0.5)			
18.60	0.042		0.10			(0.5)			
19.05	0.18 (2)	0.563	120 (30)	0	4	0.32	120 (20)	90 (10)	137
21.88	0.38 (4)	0.438	200 (30)	0	3	0.87	130 (15)	150 (40)	139
22.92	0.17								
23.00	0.51 (5)	0.438	700 (100)	0	3	1.16	420 (60)	700 (100)	457
25.84	0.14								
27.56	0.42 (8)	0.563	420 (60)	0	4	0.75		420 (50)	363
28.31	0.11								
28.64	0.038 (6)					(0.5)			
29.4								$2g\Gamma_n$ = 160	
29.63	0.085 (6)								
29.80	0.093								
31.58	0.64		30 (15)			1.35			
32.4	0.47 (23)	0.563	1000 (500)	0	4	0.83		2000 (200)	821
34.11	0.037 (9)					(0.5)			
35.32	0.089 (9)					(0.5)			
35.6								$2g\Gamma_n$ = 142	
36.18	0.11 (1)								
36.70	0.15 (3)		400 (100)			0.29			
36.97	0.09 (1)								
38.93	0.73 (21)	0.563	1500 (200)	0	4	1.30		1700 (200)	1403

(Continued)

TABLE 9 (cont'd)

E_n [a] (keV)	$g\Gamma_\gamma\Gamma_n/\Gamma$ [b] (eV)	g [c]	Γ_n [d] (eV)	ℓ	J [c]	Γ_γ [e] (eV)	Γ_n [g]
42.51	0.15						
42.72	0.06 (15)						
43.45	0.19						
44.01	0.14 (1)						
45.95	0.15 (1)						
49.72	0.15 (1)						
50.20	0.061 (15)						
50.46	0.33						
51.45	0.11 (2)		200 (50)			0.22	
51.97	0.06 (3)						
53.20	0.43						
56.82	0.44 (17)	0.563	600 (150)	0	4	0.79	450 (100)
58.40	0.18						
58.72	0.069 (14)						
59.13	0.067 (12)						
60.07	0.26 (2)	0.438	390 (80)	0	3	0.60	450 (100)
60.34	0.29						
62.10	0.057 (15)						
63.22	0.30 (2)		200 (100)				
63.43	0.18						
67.6	0.29 (10)	0.438	800 (300)	0	3	0.66	800 (100)
68.10	0.15 (2)						
72.00	0.12 (2)						
72.20	0.18						
72.75	0.26						
76.70	0.81 (26)	0.563	1000 (200)			1.4	900 (200)
77.92	0.39 (3)						
78.35	0.27 (3)						

TABLE 9 (cont'd)

a) Systematic energy error 0.2%. Relative energy error $\lesssim$ 0.1 unless the least significant error is given in parentheses.

b) Error in least significant figure is given in parentheses if > 5% (*e.g.* 2.05 (110) ≡ 2.05±1.10). Normalisation error of 12% is not included.

c) g and J values from Cho *et al.*]1970], otherwise g=0.5 assumed. J=4 for 3.827 keV resonance from comparison with $g\Gamma_n$.

d) When Γ_n is not specified, Γ_n = 5 eV above 20 keV is assumed for self-shielding calculation. Γ_n values given are independent of g when $\Gamma_n >> \Gamma_\gamma$.

e) When $\Gamma_n << \Gamma_\gamma$, Γ_γ = 0.5 eV is assumed.

f) Good (cited in Mughabghab & Garber [1973])

g) Cho *et al.* [1970] or Muller & Rohr [1971].

h) Good *et al.* [1966].

TABLE 10

^{50}Ti RESONANCE PARAMETERS

E_n [a] (keV)	$g\Gamma_\gamma\Gamma_n/\Gamma$ [b] (eV)	$g\Gamma_n$ [c] (eV)	ℓ [d]	J [d]	$g\Gamma_n$ [e] (eV)	$g\Gamma_n$ [f] (eV)	$g\Gamma_n$ [g] (eV)
16.99	0.15						
54.38	0.23 (2)						
56.50	1.10 (30)	900 (200)	0	$^1/_2$	900	900	870 (90)
60.78	0.89						
73.55	0.71						
76.50	0.17 (4)	(77)					77
78.75	2.27						
81.68	0.18 (3)						
84.55	0.11 (5)	(108)					108
87.38	0.51 (3)						
90.1						990	
92.9							135
97.60	0.77 (6)	(116)					
100.0							116
101.4	0.16 (4)						
120.6	0.57 (4)	(139)					139
146.8	-		0	$^1/_2^+$	420		
188.0	-		0	$^1/_2$		1500	
185.6	-		0	$^1/_2$	1520		
194.0	-						265
225.1	0.42 (16)	(253)					253
227.0	-						274
233.5	0.25 (25)	(190)					190
245.0							236
248.0							172
250.5	0.67 (18)	(221)					221
252.6	0.78 (20)	(136)					136
257.9	0.74 (21)	(174)					174
290.3	1.92 (34)	(82)					82

TABLE 10 (cont'd)

a) Systematic energy error 0.2%. Relative energy error $\lesssim$ 0.1% unless the least significant error is given in parentheses.

b) Error in least significant figure is given in parentheses if > 5% (e.g. 2.05 (110) $\equiv$ 2.05±1.10). Normalisation error of 12% is not included.

c) $g\Gamma_n$ values in parenthesis are assumed; when not specified $g\Gamma_n$ = 5 eV are assumed.

d) ℓ,J values from Farrell *et al.* [1966], Garg *et al.* [1971] and Good (cited in Mughabghab & Garber [1973].

e) Farrell *et al.* [1966]

f) Garg *et al.* [1971]

g) Good (cited in Mughabghab & Garber [1973].

TABLE 11

s-WAVE VALENCE PARAMETERS

A	E_λ (keV)	$\Gamma^0_{\lambda n}$ (eV)	$10^2 Q_\lambda$	$\Gamma^V_{\lambda\gamma}$ (eV)	$\Gamma_{\lambda\gamma}$ (eV)
^{46}Ti	11.07	0.76	9.22	0.07	0.49
	39.2	1.26	8.55	0.11	0.67
	48.7	6.80	8.36	0.57	1.03
	63.2	13.9	8.08	1.12	1.96
	100.0	15.2	7.32	1.11	3.70
	178.9	3.07	5.61	0.17	2.21
^{47}Ti	3.090	1.80	11.78	0.212	1.09
	4.192	0.03	11.78	0.004	0.53
	8.130	0.44	8.4	0.037	0.62
	8.338	0.88	8.2	0.072	1.43
	10.54	0.54	11.5	0.062	1.21
	12.12	1.09	11.5	0.126	1.29
	12.14	0.20	8.2	0.016	0.92
	12.83	1.41	8.2	0.116	1.87
	16.36	2.35	11.5	0.270	0.94
	17.42	0.30	7.9	0.024	1.75
	19.09	0.15	11.2	0.017	0.97
	21.29	0.42	7.9	0.033	1.50
	27.20	5.22	11.2	0.585	2.56
	30.23	0.37	7.7	0.028	0.78
	32.61	3.32	7.7	0.256	0.85
	37.04	2.60	(9.2)	(0.24)	0.73
	38.12	0.51	10.7	0.055	0.58
	40.55	3.47	10.7	0.371	2.03
	41.06	0.29	7.6	0.022	0.28
	42.36	1.94	7.6	0.147	2.26
	46.30	1.39	10.4	0.145	2.53
	49.32	0.90	10.4	0.094	1.82

TABLE 11 (cont'd)

A	E (keV)	$\Gamma^0_{\lambda n}$ (eV)	$10^2 Q_\lambda$	$\Gamma^V_{\lambda\gamma}$ (eV)	$\Gamma_{\lambda\gamma}$ (eV)
^{48}Ti	17.6	65.6	8.27	5.43	2.3
	22.10	4.37	8.18	0.36	0.8
	36.8	6.52	7.92	0.52	2.5
	51.9	10.4	7.57	0.79	1.4
	83.48	0.45	6.96	0.03	0.61
	119.2	0.58	6.35	0.04	0.52
	153.7	1.01	5.74	0.06	2.75
	191.4	4.57	5.05	0.23	0.89
^{49}Ti	3.83	3.22	11.8	0.38	0.52
	8.44	2.72	(10)	(0.27)	0.58
	19.04	0.725	11.1	0.08	0.32
	21.88	1.35	8.62	0.12	0.87
	23.00	4.62	8.62	0.40	1.16
	27.56	2.41	10.9	0.26	0.75
	32.4	8.33	10.9	0.91	0.83
	38.93	7.60	10.6	0.81	1.30
	56.83	2.52	10.4	0.26	0.79
	60.08	1.59	7.89	0.13	0.60
	67.60	3.08	7.79	0.24	0.66
	76.70	3.61	9.68	0.35	1.4
^{50}Ti	56.5	3.78	5.92	0.23	1.10

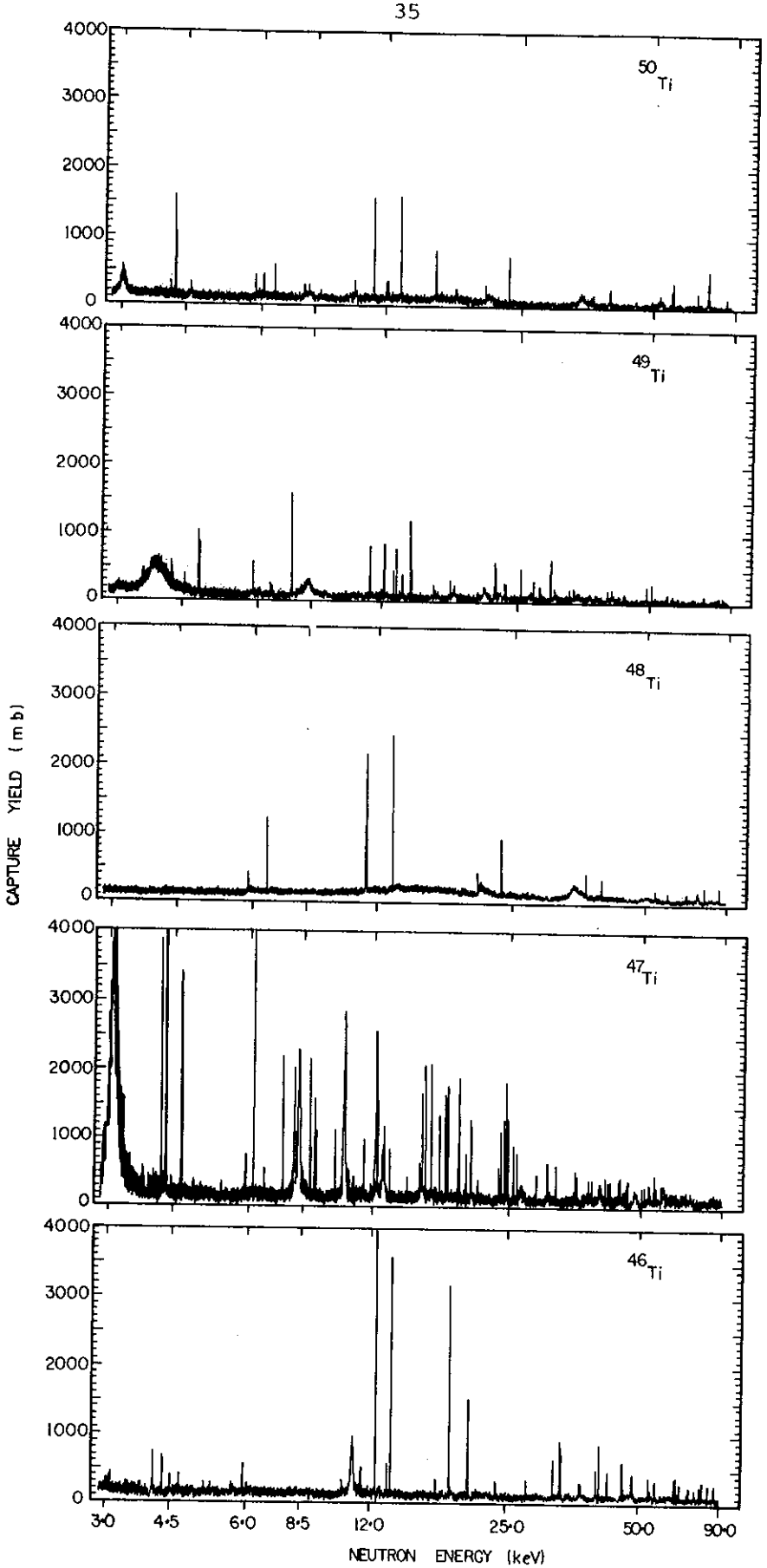

FIGURE 1. CAPTURE YIELD (mb) FOR THE Ti ISOTOPES IN THE ENERGY RANGE 3 TO 90 keV

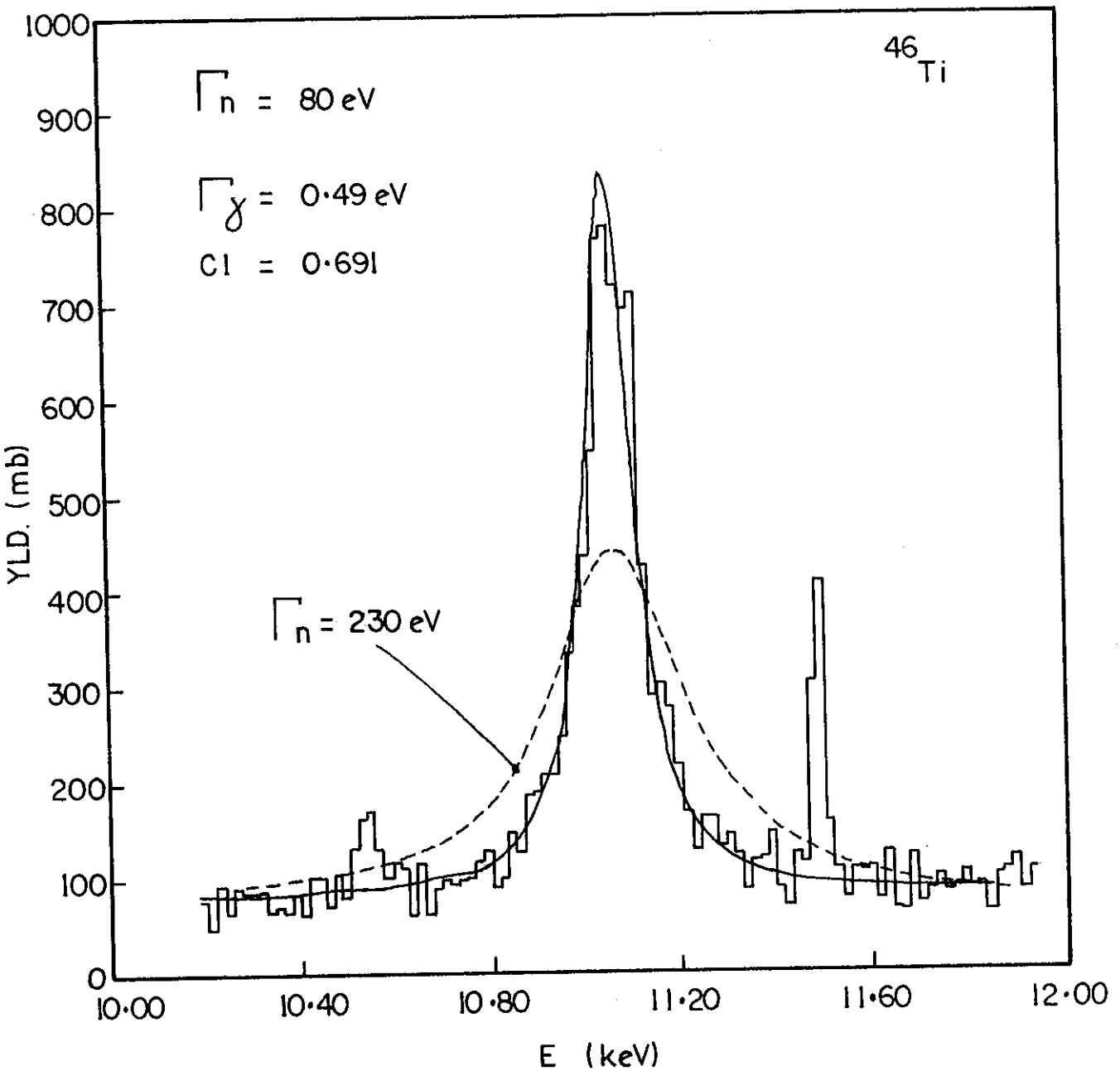

FIGURE 2. 11.1 keV s-WAVE RESONANCE IN ^{46}Ti. THE CALCULATED SELF SHIELDING FACTOR IS GIVEN BY CI.

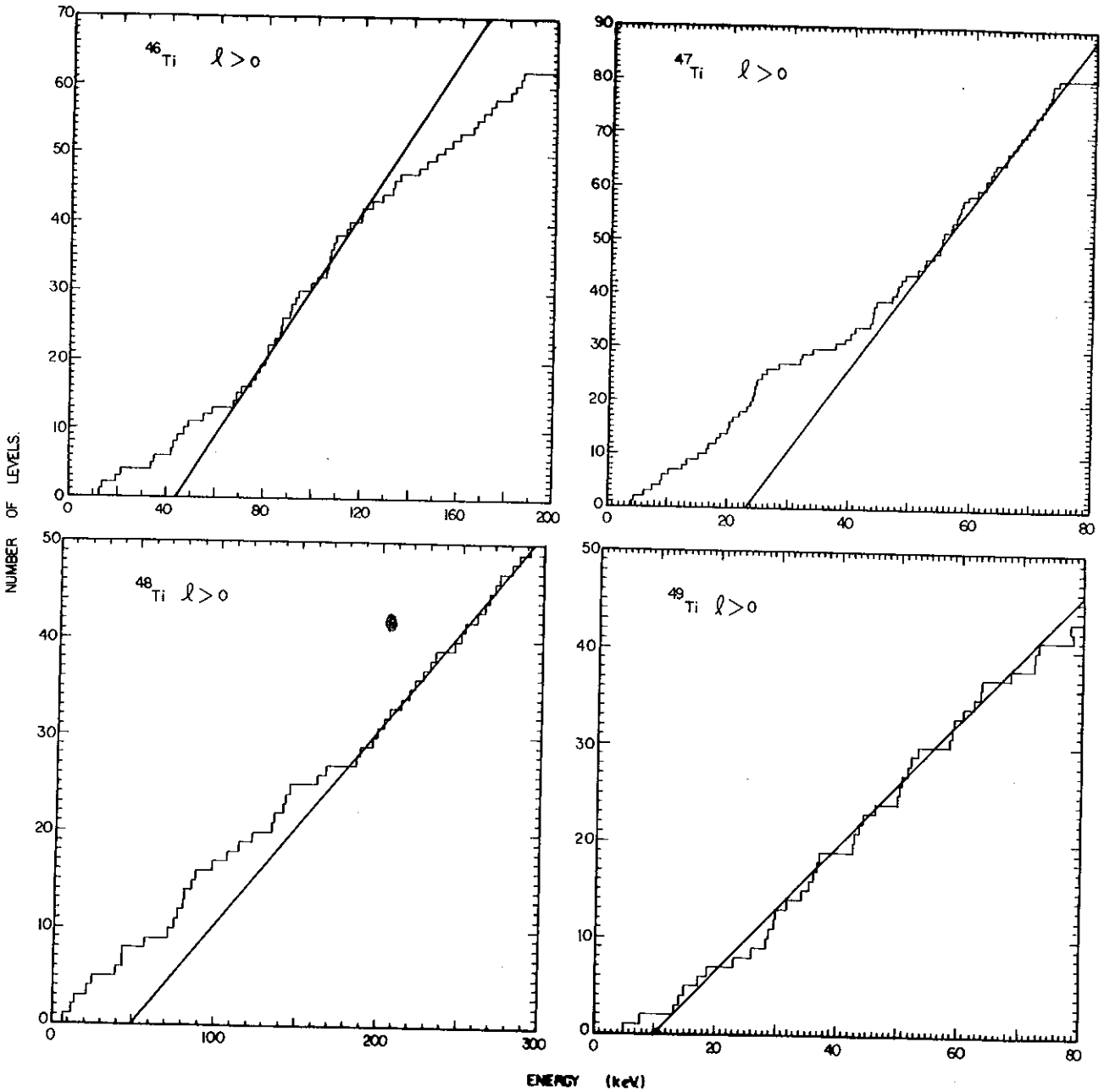

FIGURE 3. OBSERVED $\ell > 0$ LEVEL DENSITIES

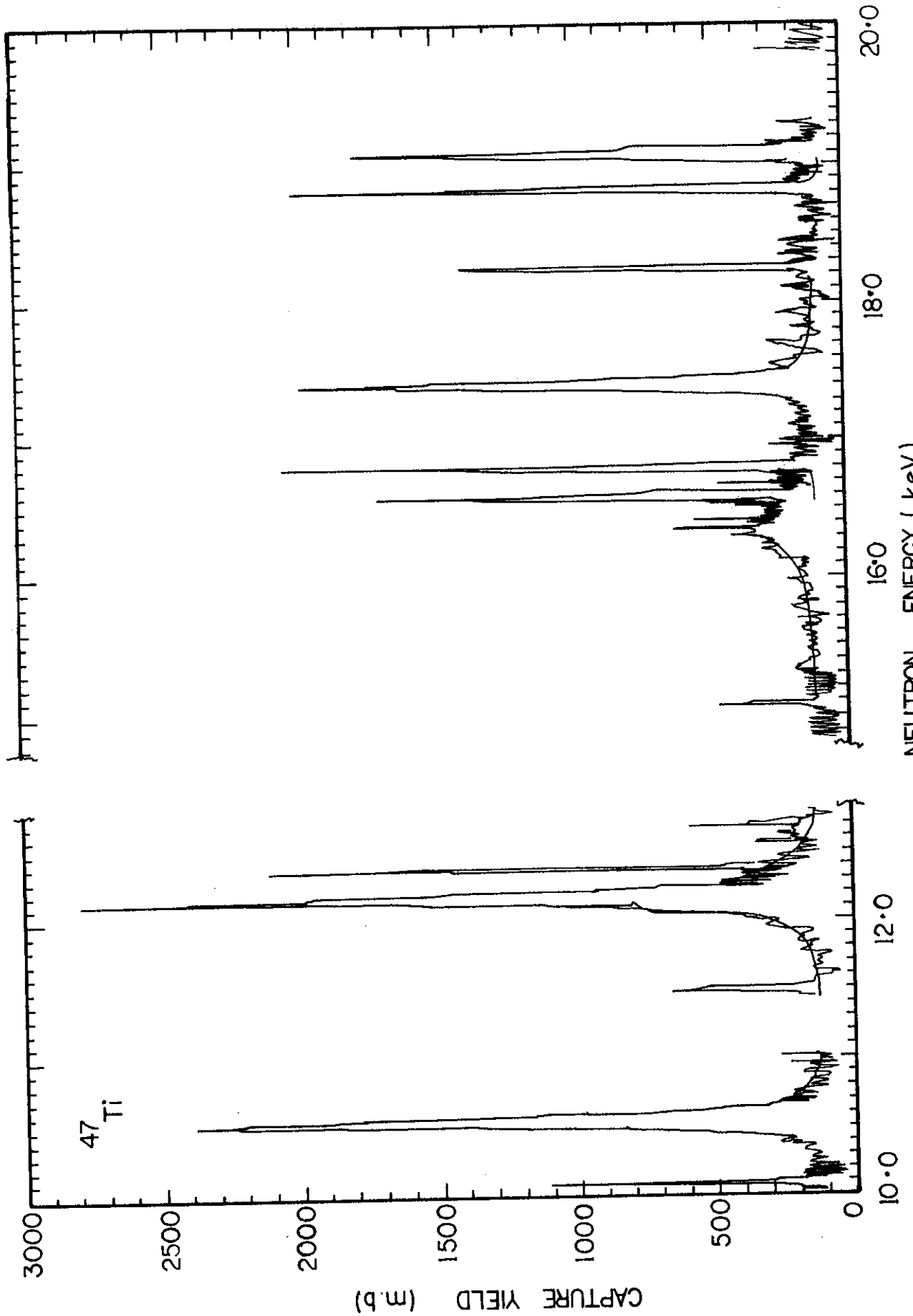

FIGURE 4. CAPTURE YIELD IN ^{47}Ti FROM 10 TO 20 keV

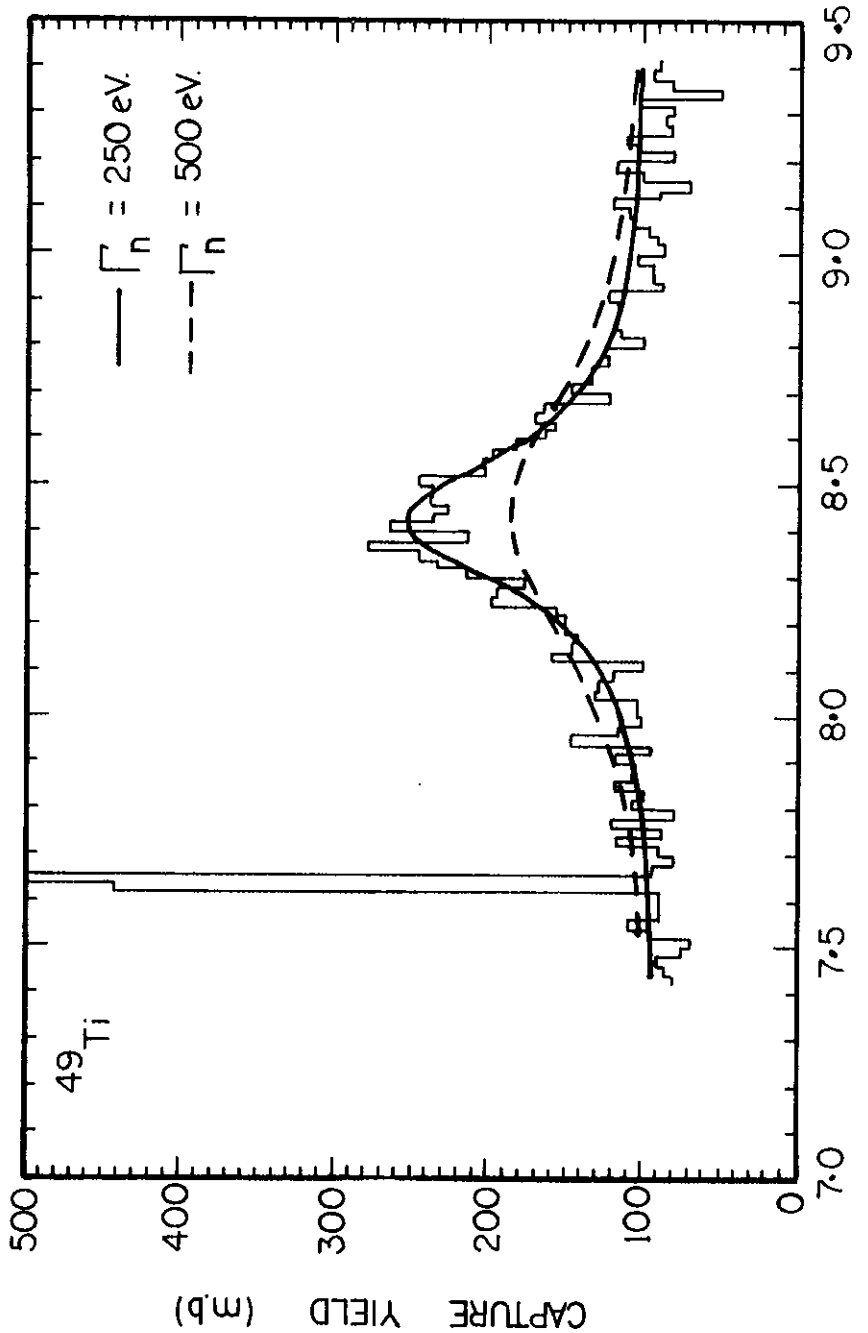

FIGURE 5. 8.44 keV s-WAVE RESONANCE IN ^{49}Ti